Synthesis of Double-End-Capped Polyethylene by a Cationic Tris(pyrazolyl)borate Zirconium Benzyl Complex

Katrin Nienkemper, Han Lee, Richard F. Jordan,* Alireza Ariafard, Li Dang, and Zhenyang Lin*

Department of Chemistry, The University of Chicago, 5735 South Ellis Avenue, Chicago, Illinois 60637, and Department of Chemistry, The Hong Kong University of Science and Technology, Clear Water Bay, Kowloon, Hong Kong

Received June 16, 2008

The cationic complexes Tp*Zr$(CH_2Ph)_2^+$ (**I**, $B(C_6F_5)_4^-$ salt; Tp* = HB(3,5-Me_2-pyrazolyl)$_3$) and {$(PhCH_2)$(H)B(μ-Me_2pz)$_2$}Zr(η^2-Me_2pz)$(CH_2Ph)^+$ (**II**; Me_2pz = 3,5-Me_2-pyrazolyl) polymerize ethylene at −78 to −60 °C to linear polyethylene (PE) without significant chain transfer. For **I**, chain growth takes place at only one benzyl group. Quenching these polymerizations with MeOH yields benzyl-capped PE ($PhCH_2(CH_2CH_2)_nCH_2CH_3$). Quenching **I**-catalyzed ethylene polymerization with Br_2 yields double-end-capped PE containing benzyl and bromo chain ends ($PhCH_2(CH_2CH_2)_nCH_2CH_2Br$). DFT calculations on model catalysts show that ethylene insertion into a Zr−η^2-CH_2Ph bond requires greater structural distortion than insertion into a Zr−$CH_2CH_2CH_2Ph$ bond. The calculations also show that the β-H transfer to monomer and β-H elimination chain transfer pathways are both strongly disfavored for **I**, but the β-H transfer to monomer path may be possible for **II**.

Introduction

Group 4 metal Tp′MCl_3 tris(pyrazolyl)borate complexes (Tp′ = generic tris(pyrazolyl)borate) can be activated by methylalumoxane (MAO) to produce highly active olefin polymerization catalysts.[1−4] The dominant chain transfer mechanism in ethylene polymerization by many Tp′MCl_3/MAO catalysts is chain transfer to MAO and the $AlMe_3$ contained therein. Therefore, molecular weight can be controlled by varying the alkyl aluminum concentration, and Al-terminated polymers, which are useful for the synthesis of functional polymers and block copolymers, can be obtained.[1] β-H transfer is usually insignificant for these catalysts. These results suggest that *Al-free* group 4 metal Tp′M-based catalysts may exhibit characteristics of living polymerization.[5]

The identity of the active species in Tp′MCl_3/MAO catalysts is unknown, and the chemistry of group 4 metal Tp′M alkyls is virtually unexplored.[6−8] However, by analogy with Cp_2MCl_2/MAO metallocene catalysts, in which Cp_2MR^+ cations are the active species, the active species in Tp′MCl_3/MAO systems may be Tp′MR_2^+ cations. We recently developed routes to neutral and cationic Tp*Zr benzyl complexes (Tp* = HB(3,5-Me_2-pyrazolyl)$_3$).[9] As shown in Scheme 1, Tp*Zr$(CH_2Ph)_3$ can be prepared by the reaction of K[Tp*] with Zr$(CH_2Ph)_4$.[10] The reaction of Tp*Zr$(CH_2Ph)_3$ with [Ph_3C][$B(C_6F_5)_4$] at −60 °C yields the cationic complex Tp*Zr$(CH_2Ph)_2^+$ (**I**, $B(C_6F_5)_4^-$ salt). Cation **I** rearranges to {$(PhCH_2)$(H)B(μ-Me_2pz)$_2$}Zr(η^2-Me_2pz)$(CH_2Ph)^+$ (**II**) at 0 °C by net exchange of a Zr-*CH_2Ph* group and a B-*pz** group (pz* = 3,5-Me_2-pyrazolyl).[11] Complexes **I** and **II** both polymerize ethylene rapidly at −60 °C in CD_2Cl_2 to linear polyethylene (PE). Here we report experimental and computational results that show that these polymerizations

* Corresponding authors. E-mail: rfjordan@uchicago.edu; chzlin@ust.hk.

(1) (a) Murtuza, S., Jr.; Jordan, R. F. *Organometallics* **2002**, *21*, 1882. (b) Michiue, K.; Jordan, R. F. *Macromolecules* **2003**, *36*, 9707. (c) Michiue, K.; Jordan, R. F. *Organometallics* **2004**, *23*, 460. (d) Michiue, K.; Jordan, R. F. *J. Mol. Catal. A* **2008**, *282*, 107.

(2) (a) Gil, M. P., Jr. *Appl. Catal., A* **2007**, *332*, 110. (b) Gil, M. P.; dos Santos, J. H. Z.; Casagrande, O. L., Jr. *J. Mol. Catal. A* **2004**, *209*, 163. (c) Furlan, L. G.; Gil, M. P.; Casagrande, O. L., Jr. *Macromol. Rapid Commun.* **2000**, *21*, 1054. (d) Gil, M. P.; Casagrande, O. L., Jr. *J. Organomet. Chem.* **2004**, *689*, 286. (e) Gil, M. P.; dos Santos, J. H. Z.; Casagrande, O. L., Jr. *Macromol. Chem. Phys.* **2001**, *202*, 319.

(3) Nakazawa, H.; Ikai, S.; Imaoka, K.; Kai, Y.; Yano, T. *J. Mol. Catal. A* **1998**, *132*, 33.

(4) (a) Karam, A.; Jimeno, M.; Lezama, J.; Catari, E.; Figueroa, A.; de Gascue, B. R. *J. Mol. Catal. A* **2001**, *176*, 65. (b) Karam, A.; Casas, E.; Catari, E.; Pekerar, S.; Albornoz, A.; Mendez, B. *J. Mol. Cat. A* **2005**, *238*, 233. (c) Karam, A.; Pastran, J.; Casas, E.; Mendez, B. *Polym. Bull.* **2005**, *55*, 11. (d) Casas, E.; Karam, A.; Diaz-Barrios, A.; Albano, C.; Sanchez, Y.; Mendez, B. *Macromol. Symp.* **2007**, *257*, 131.

(5) (a) Sakuma, A.; Weiser, M.; Fujita, T. *Polym. J.* **2007**, *39*, 193. (b) Domski, G. J.; Rose, J. M.; Coates, G. W.; Bolig, A. D.; Brookhart, M. *Prog. Polym. Sci.* **2007**, *32*, 30. (c) Furuyama, R.; Saito, J.; Ishii, S.; Makio, H.; Mitani, M.; Tanaka, H.; Fujita, T. *J. Organomet. Chem.* **2005**, *690*, 4398. (d) Coates, G. W.; Hustad, P. D.; Reinartz, S. *Angew. Chem., Int. Ed.* **2002**, *41*, 2236. (g) Doi, Y.; Keii, T. *Adv. Polym. Sci.* **1986**, *73−74*, 201.

(6) (a) Reger, D. L.; Tarquini, M. E.; Lebloda, L. *Organometallics* **1983**, *2*, 1763. (b) Ipaktschi, J.; Sulzbach, W. J. *J. Organomet. Chem.* **1992**, *426*, 59.

(7) For group 4 metal alkyl complexes containing tridentate bis(pyrazolyl)-phenoxide ligands see: (a) Cuomo, C.; Milione, S.; Grassi, A. *Macromol. Rapid Commun.* **2006**, *27*, 611. (b) Milione, S.; Cuomo, C.; Grassi, A. *Top. Catal.* **2006**, *40*, 163. (c) Milione, S.; Bertolasi, V.; Cuenca, T.; Grassi, A. *Organometallics* **2005**, *24*, 4915. (d) Howe, R. G.; Tredget, C. S.; Lawrence, S. C.; Subongkoj, S.; Cowley, A. R.; Mountford, P. *Chem. Commun.* **2006**, 223.

(8) For recent work on other group 4 metal scorpionate complexes see: (a) Dunne, J. F.; Su, J.; Ellern, A.; Sadow, A. D. *Organometallics* **2008**, *27*, 2399. (b) Cai, H.; Lam, W. H.; Yu, X.; Liu, X.; Wu, Z.; Chen, T.; Lin, Z.; Chen, X.; You, X.; Xue, Z. *Inorg. Chem.* **2003**, *42*, 3008. (c) Gazzi, R.; Perazzolo, F.; Sostero, S.; Ferrari, A.; Traverso, O. *J. Organomet. Chem.* **2005**, *690*, 2071. (d) Bigmore, H. R.; Dubberley, S. R.; Kranenburg, M.; Lawrence, S. C.; Sealey, A. J.; Selby, J. D.; Zuideveld, M. A.; Cowley, A. R.; Mountford, P. *Chem. Commun.* **2006**, 436.

(9) Lee, H.; Jordan, R. F. *J. Am. Chem. Soc.* **2005**, *127*, 9384.

(10) For a similar synthesis of Tp′AlR_2 compounds see: Looney, A.; Parkin, G. *Polyhedron* **1990**, *9*, 265.

(11) For a similar rearrangement of Tp*$_2$Sm(C≡CPh) see: Lin, G.; McDonald, R.; Takats, J. *Organometallics* **2000**, *19*, 1814.

10.1021/om800558w CCC: $40.75 © 2008 American Chemical Society
Publication on Web 10/22/2008

Scheme 1[a]

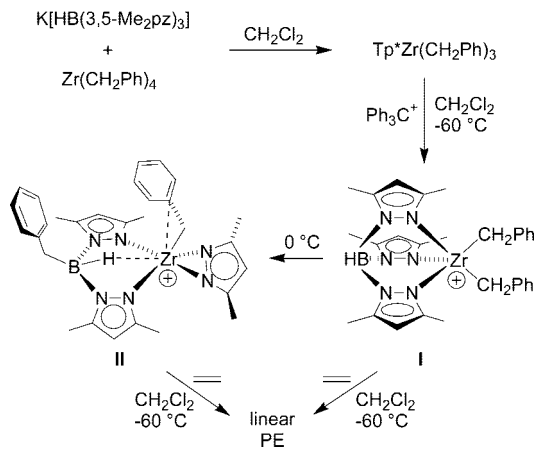

[a] Anion = $B(C_6F_5)_4^-$.

Scheme 2

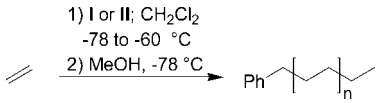

proceed without significant chain transfer at low temperature and can be used to prepare double-end-capped PE.

Results and Discussion

NMR Scale Ethylene Polymerizations. Complex **I** was generated from Tp*Zr(CH_2Ph)$_3$ and [Ph_3C][$B(C_6F_5)_4$] on an NMR scale in CD_2Cl_2 and reacted with ethylene (40 equiv) at −78 to −60 °C (Scheme 2). ^{1}H NMR analysis showed that **I** consumed all of the available ethylene within 10 min, PE was formed, and 35% of the starting **I** remained unreacted. The reaction was quenched with MeOH at −78 °C, and the PE was isolated by filtration. NMR analysis showed that the PE was linear and contained approximately one benzyl end group per methyl end group. The ratio of the integrals of the $-CH_2CH_2Ph$ ^{1}H resonance (δ 2.65, t) to the $-CH_2CH_3$ resonance (δ 0.92, t) was 2:3.2.[12] Olefin resonances were not observed. In addition, the number average molecular weight of the PE determined by ^{1}H NMR ($M_{n,NMR}$) agreed well with the value ($M_{n,calcd}$) predicted assuming that each molecule of **I** that reacts with ethylene produces one polymer chain by insertion into only one Zr−CH_2Ph bond and that chain transfer does not occur ($M_{n,NMR}$ = 2000, $M_{n,calcd}$ = 1800).

Similar results were obtained with **II** (Scheme 2). A solution of **II** in CD_2Cl_2 was generated by warming a CD_2Cl_2 solution of **I** to 0 °C for 10 min and then reacted with ethylene (50 equiv) at −78 to −60 °C. **II** consumed all of the available ethylene within 10 min and 26% of the starting **II** remained unreacted. Linear PE with about one benzyl end group per methyl end group was produced. The $M_{n,calcd}$ (2000) and $M_{n,NMR}$ (2600) values were similar.

These experiments suggest that **I** and **II** polymerize ethylene without significant chain transfer at −78 to −60 °C and imply that in both cases the first insertion (initiation) is slower than subsequent insertions (growth). For **I**, chain growth takes place at only one benzyl group.

Scheme 3

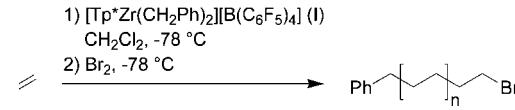

Synthesis of Double-End-Capped Polyethylene. Larger scale ethylene polymerizations were conducted with catalyst **I** using Br_2 as the quenching agent to produce double-end-capped PE, $PhCH_2(CH_2CH_2)_nCH_2CH_2Br$, as shown in Scheme 3.[13] **I** was generated in CH_2Cl_2 at −78 °C and then reacted with ethylene (1 atm on demand). Polymerization proceeded rapidly and was quenched by addition of excess Br_2 after ca. 2 min to produce $PhCH_2(CH_2CH_2)_nCH_2CH_2Br$. Representative results are summarized in Table 1.

The ^{1}H NMR spectrum of a typical double-end-capped PE produced by Scheme 3 is shown in Figure 1. This spectrum is characteristic of a linear PE with virtually no branching or olefin groups. The spectrum contains triplets for the $-CH_2CH_2Br$ (δ 3.34) and $-CH_2CH_2Ph$ (δ 2.65) end groups in a 1:1 integral ratio.[14,15] The spectrum also contains signals for $-CH_2CH_2Br$ (δ 1.85) and $-CH_2CH_2Ph$ (δ 1.69) penultimate units in a 1:1 integral ratio.[16] DSC data for the PEs in Table 1 (T_m = 135−137 °C) are consistent with linear structures.

Table 1 shows that the ratio of $-CH_2CH_2Br$ to $-CH_2CH_2Ph$ chain ends is reproducibly 1:1. However, the PE yields and $M_{n,NMR}$ values are variable due to (i) minor decomposition of starting **I** due to adventitious impurities (no scavenger was used), (ii) mass transport limitations resulting from precipitation of the presumed growing [Tp*Zr(CH_2Ph){$(CH_2CH_2)_nCH_2Ph$}]-[$B(C_6F_5)_4$] species, and (iii) the fact that initiation is slower than growth under these conditions. The number of PE chains produced per Zr center ranges between 0.2 and 1.0, which is consistent with the absence of chain transfer.

These results confirm that chain transfer is insignificant in ethylene polymerization catalyzed by **I** at low temperature and that the active Zr-$(CH_2CH_2)_{n+1}CH_2Ph$ species can be quenched with Br_2 to yield $PhCH_2(CH_2CH_2)_nCH_2CH_2Br$.

Computational Results. Model Systems. The reactions of the model complexes $TpZr(CH_2Ph)_2^+$ (**1**, Tp = HB(pyrazolyl)$_3$) and {$(PhCH_2)(H)B(\mu\text{-pz})_2$}$Zr(\eta^2\text{-pz})(CH_2Ph)^+$ (**7**, pz = pyrazolyl) with ethylene were studied by DFT to probe how chain growth occurs and why chain transfer is strongly disfavored for **I** and **II**. Complexes **1** and **7** differ from **I** and **II** by replacement of the pz* groups by unsubstituted pz groups. The DFT results show that **1** and **7** react with ethylene by weak coordination followed by insertion as observed for other d^0 metal catalysts.[17,18]

(12) (a) The assignment of the $-CH_2CH_2Ph$ resonances is based on data for $CH_3(CH_2)_{10}CH_2CH_2Ph$. ^{1}H NMR ($CDCl_3$): δ 2.59 (t, J = 8 Hz, 2H, $-CH_2CH_2Ph$), 1.60 (m, 2H, $-CH_2CH_2Ph$), 1.25 (m, 20H, $-(CH_2)_{10}-$), 0.88 (t, J = 7 Hz, $-CH_2CH_3$). (b) Pilcher, A. S.; DeShong, P. *J. Org. Chem.* **1996**, *61*, 6901.

(13) (a) Iodide-terminated polypropylene: Doi, Y.; Watanabe, Y.; Ueki, S.; Soga, K. *Makromol. Chem., Rapid Commun.* **1983**, *4*, 533. (b) Doi, Y.; Hizal, G.; Soga, K. *Makromol. Chem.* **1987**, *188*, 1273. (c) Aryl- and silyl-functionalized PE: Brookhart, M.; DeSimone, J. M.; Grant, B. E.; Tanner, M. J. *Macromolecules* **1995**, *28*, 5378. (d) Thienyl-capped PE: Ringelberg, S. N.; Meetsma, A.; Hessen, B.; Teuben, J. H. *J. Am. Chem. Soc.* **1999**, *121*, 6082.

(14) The assignment of the $-CH_2CH_2Br$ resonances is based on data for $CH_3(CH_2)_9CH_2CH_2Br$. ^{1}H NMR (*o*-dichlorobenzene-d_4): δ 3.31 (t, J = 7 Hz, 2H, $-CH_2CH_2Br$), 1.82 (quint, J = 7 Hz, 2H, $-CH_2CH_2Br$), 1.31 (s, 18H, $-(CH_2)_9-$), 0.92 (t, J = 7 Hz, 3H, $-CH_3$).

(15) In some cases the integral ratio $I_{CH2Ph}/I_{CH2Br} > 1$ due to adventitious hydrolysis prior to quenching; in these cases $I_{CH3} + I_{CH2Br} \approx I_{CH2Ph}$.

(16) Some NMR spectra show a broad signal at δ 0.9, in the expected range for methyl end groups. Control experiments conclusively established that this signal is due to external impurities.

Table 1. Synthesis of Double-End-Capped Polyethylene by [Tp*Zr(CH$_2$Ph)$_2$][B(C$_6$F$_5$)$_4$] with Br$_2$ as Capping Agent (Scheme 3)[a]

run	catalyst (μmol)	[catalyst] (mM)	time (s)	PE yield (g)	$M_{n,NMR}$[b]	T_m[c] (°C)	I_{CH2Br}/I_{CH2Ph}[d]	# chains/Zr[e]
1	21.2	1.06	120	0.044	8500		1/1.0	0.24
2	21.2	1.06	100	0.090	15900	134.6	1/1.0	0.27
3	21.2	1.06	115	0.158	20500	135.1	1/0.9	0.36
4	21.2	1.06	130	0.328	21700	137.2	1/1.1	0.71
5	21.2	1.06	130	0.422	20000	136.6	1/1.0	0.99
6	10.6	0.21	185	0.020	10200	134.0	1/1.0	0.18
7	10.6	0.21	190	0.020	12600	132.7	1/1.0	0.15

[a] Conditions: catalyst: [Tp*Zr(CH$_2$Ph)$_2$][B(C$_6$F$_5$)$_4$] (**I**), generated in situ from Tp*Zr(CH$_2$Ph)$_3$ and [Ph$_3$C][B(C$_6$F$_5$)$_4$]. Solvent: 20 mL of CH$_2$Cl$_2$ for runs 1−5, 50 mL of CH$_2$Cl$_2$ for runs 6 and 7; 1 atm of ethylene; −78 °C. [b] Number average molecular weight determined by ^{1}H NMR. [c] Determined by DSC. [d] Ratio of integrals of the −C*H*$_2$Br (δ 3.34, I$_{CH2Br}$) and −C*H*$_2$Ph (δ 2.65, I$_{CH2Br}$) ^{1}H NMR resonances. [e] Number of PE chains produced per Zr = (g PE)(M$_n$)$^{-1}$(μmol Zr)$^{-1}$(10^6).

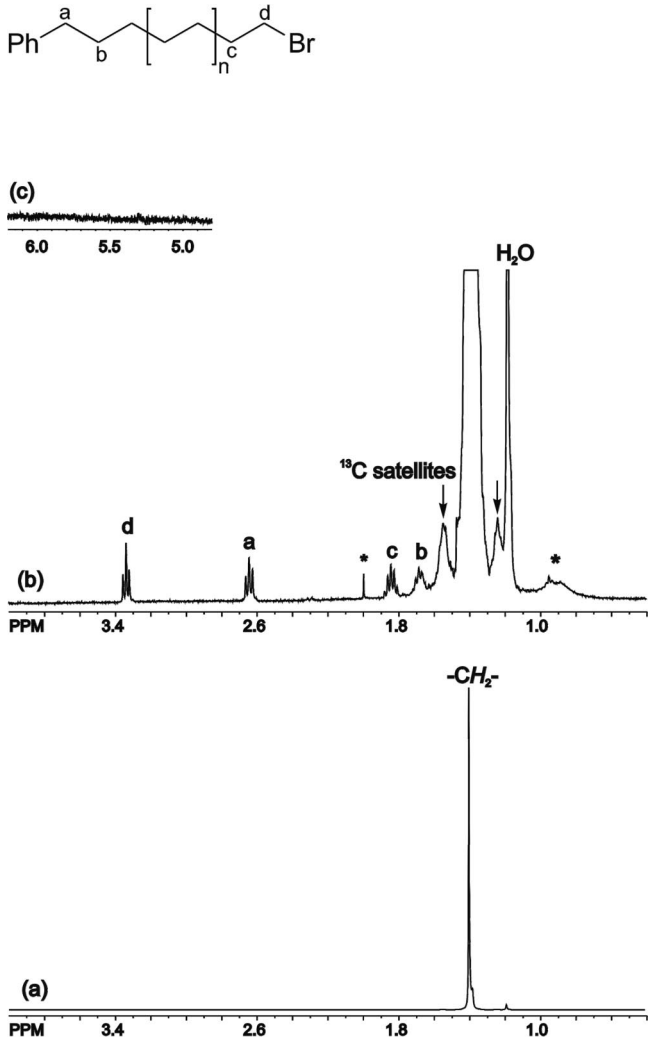

Figure 1. ^{1}H NMR spectrum of a PhCH$_2$(CH$_2$CH$_2$)$_n$CH$_2$CH$_2$Br double-end-capped polyethylene (*o*-dichlorobenzene-d_4, 120 °C). Assignments of key resonances are given on the structure at the top. Resonances due to external impurities are marked by "*". (a) Spectrum highlighting the PE main chain −C*H*$_2$− resonance. (b) Expansion highlighting the −C*H*$_2$C*H*$_2$Br and −C*H*$_2$C*H*$_2$Ph resonances. (c) Expansion of the olefin region showing the absence of significant olefin resonances.

Chain Growth. The potential energy profile for the first two ethylene insertions of **1** is shown in Figure 2, and structural data for key species are provided in Figure 3.[19] **1** binds ethylene very weakly (ΔE = −0.9 kcal/mol) to form adduct **2**. The average Zr−C(ethylene) distance in **2** is very long (3.9 Å) and the Zr−η^2-benzyl interactions are not significantly perturbed versus the structure of **1**.[20] **2** has a distorted O_h structure and the ethylene C═C bond is parallel to the Zr−C bond of one benzyl ligand (C1). Adduct **2** undergoes insertion via migration of the C1 benzyl with a barrier of 15.0 kcal/mol to form **3**. **3** contains a nonagostic alkyl ligand. Overall, the first insertion (**1** → **3**) is exothermic by 16.8 kcal/mol. **3** also coordinates ethylene weakly to form adduct **4**, which is structurally similar to **2** and undergoes insertion into the Zr−CH$_2$CH$_2$CH$_2$Ph bond to generate **5**. The second insertion has a much lower barrier (**4** → **5**, 11.4 kcal/mol) and is more exothermic (**3** → **5**, ΔE = −23.0 kcal/mol) than the first insertion. Alternatively, as shown in Figure 4, **4** could undergo insertion into the Zr−CH$_2$Ph bond to generate TpZr(CH$_2$CH$_2$CH$_2$Ph)$_2^+$ (**6**), which contains two growing polymeryl chains. However, the conversion of **4** to **6** has a higher barrier (15.4 kcal/mol) and is less exothermic (ΔE = −13.6 kcal/mol) than the conversion of **4** to **5**. These results are consistent with the experimental observation that **I** undergoes slow ethylene insertion into a Zr−CH$_2$Ph bond followed by faster insertion into the resulting Zr−CH$_2$CH$_2$CH$_2$Ph bond.

The potential energy profile for the first two ethylene insertions of **7** is shown in Figure 5, and structural data for key species are provided in Figure 6. Complex **7** binds ethylene to form **8**. The average Zr−C(ethylene) distance in **8** (3.1 Å) is much shorter than those in **2** and **4**. However, coordination of ethylene to **7** to generate **8** weakens the Zr−η^2-benzyl interaction (see Figure 6), so the net binding energy is again low (ΔE = −0.7 kcal/mol). The computed structures of **7** and **8** are very similar to the structures of **I** and the PMe$_3$ adduct **I**·PMe$_3$ determined by X-ray crystallography.[9] A similar weakening of the Zr−η^2-benzyl interaction was observed upon binding of

(17) (a) Castonguay, L. A.; Rappé, A. K. *J. Am. Chem. Soc.* **1992**, *11*, 5832. (b) Woo, T. K.; Fan, L.; Ziegler, T. *Organometallics* **1994**, *13*, 432. (c) Margl, P.; Deng, L.; Ziegler, T. *Organometallics* **1998**, *17*, 933. (d) Margl, P.; Deng, L.; Ziegler, T. *J. Am. Chem. Soc.* **1999**, *121*, 154. (e) Rappé, A. K.; Skiff, W. A.; Casewit, C. J. *Chem. Rev.* **2000**, *100*, 1391. (f) Niu, S.; Hall, M. B. *Chem. Rev.* **2000**, *100*, 353. (g) Vyboishchikov, S. F.; Musaev, D. G.; Froese, R. D. J.; Morokuma, K. *Organometallics* **2001**, *20*, 309.

(18) (a) Lanza, G.; Fragalà, I. L.; Marks, T. J. *J. Am. Chem. Soc.* **1998**, *120*, 8257. (b) Fusco, R.; Longo, L.; Proto, A.; Masi, F.; Garbassi, F. *Macromol. Rapid Commun.* **1998**, *19*, 257. (c) Bernardi, F.; Bottoni, Z.; Miscione, G. P. *Organometallics* **1998**, *17*, 16. (d) Chan, M. S. W.; Vanka, K.; Pye, C. C.; Ziegler, T. *Organometallics* **1999**, *18*, 4624. (e) Chan, M. S. W.; Ziegler, T. *Organometallics* **2000**, *19*, 5182. (f) Nifant'ev, I. E.; Ustynyuk, L. Y.; Laikov, D. N. *Organometallics* **2001**, *20*, 5375. (g) Schaper, F.; Geyer, A.; Brintzinger, H. H. *Organometallics* **2002**, *21*, 473.

(19) The figures provide electronic energies for key species and transition states. Entropy contributions should not strongly influence the relative barriers of the first and subsequent ethylene insertions of **1** and **7** (or **I** and **II**), since these reactions involve similar species and are unimolecular. The B(C$_6$F$_5$)$_4^-$ anion was not included in the calculations. It is expected that ion pairing of the sterically crowded cations **1** and **7** (or **I** and **II**), which have coordination numbers of five or greater, with this weakly coordinating anion will be weak and will exert a similar effect on their ethylene insertion barriers.

(20) Much shorter Zr−C(olefin) distances (2.6−2.9 Å) were observed in (C$_5$R$_5$)$_2$Zr(OCMe$_2$CH$_2$CH$_2$CH═CH$_2$)$^+$ chelated olefin complexes: Carpentier, J.-F.; Wu, Z.; Lee, C. W.; Strömberg, S.; Christopher, J. N.; Jordan, R. F. *J. Am. Chem. Soc.* **2000**, *122*, 7750.

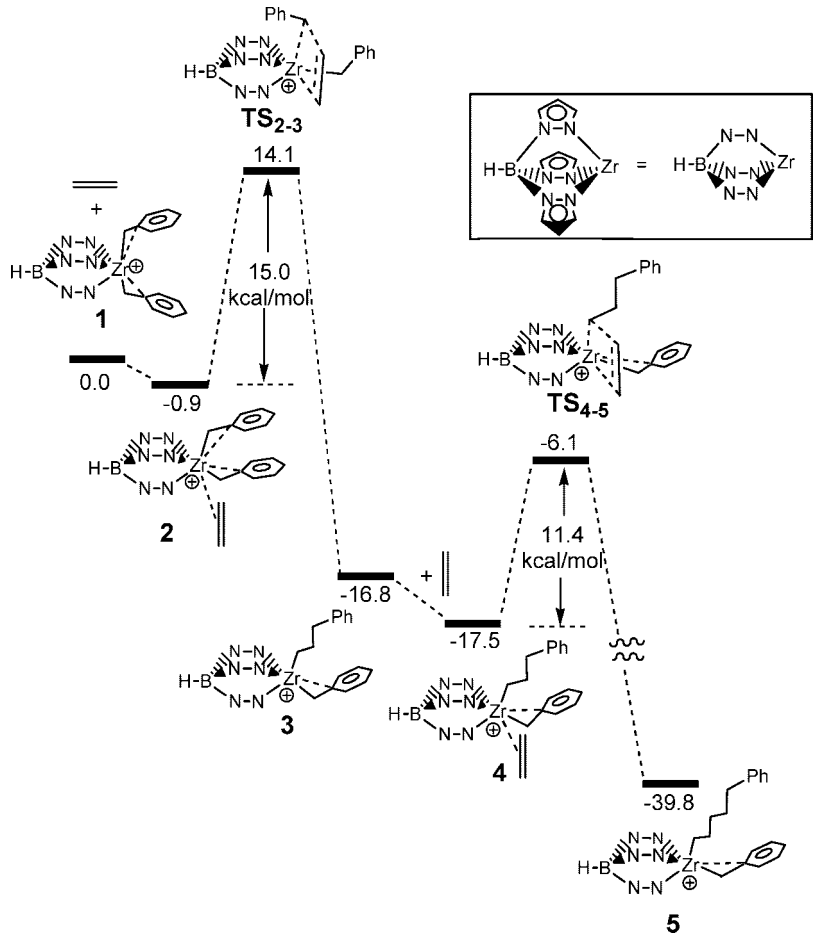

Figure 2. Calculated energy profile for the first two ethylene insertions of model complex **1**. The relative electronic energies are given in kcal/mol.

PMe_3 to **I**.[9] **8** undergoes insertion to form **9** with a barrier of 11.3 kcal/mol. **9** is structurally similar to **7** and contains a nonagostic alkyl ligand. **9** coordinates ethylene to form **10**. The average Zr−C(ethylene) distance in **10** (3.0 Å) is similar to that in **8**, but the binding energy is higher (3.4 kcal/mol) since little structural reorganization is required for ethylene coordination in this case. The insertion of **10** to form **11** has a lower barrier and is more exothermic than the conversion of **8** to **9**. These results are consistent with the experimental observation that the first ethylene insertion of **II** is slower than subsequent insertions.

The results in Figures 2−5 show that ethylene insertions into Zr−η^2-CH_2Ph bonds (**1** → **3**, **3** → **6**, and **7** → **9**) are less exothermic than insertions into Zr−$CH_2CH_2CH_2Ph$ bonds (**3** → **5** and **9**→**11**). Ethylene insertion into a Zr−C(benzyl) bond results in cleavage of the Zr−C(benzyl) bond and the ethylene π-bond and formation of benzyl−C(alkyl) and Zr−C(alkyl) bonds. Ethylene insertion into a Zr−$CH_2CH_2CH_2Ph$ bond results in cleavage of the Zr−C(alkyl) bond and the ethylene π-bond and formation of C(alkyl)−C(alkyl) and Zr−C(alkyl) bonds. These bond energies can be compared using the isodesmic reactions in eq 1−3. The reaction energy for eq 1 ($\Delta E(1)$) shows that the C(alkyl)−C(alkyl) bond is 13.9 kcal/mol stronger than the C(benzyl)−C(alkyl) bond.[21] The reaction energies for eqs 2 and 3 provide relative strengths of Zr−C(benzyl) and Zr−C(alkyl) bonds in $[Tp(PhCH_2)Zr\text{-}R]^+$ (**1**, **3**) and $[\{(PhCH_2)\text{-}(H)B(\mu\text{-}pz)_2\}(\eta^2\text{-}pz)Zr\text{-}R]^+$ (**7**, **9**) species. These results show that the Zr−C(alkyl) bonds are stronger than the Zr−C(benzyl) bonds by 5.8 and 1.6 kcal/mol, respectively. Therefore, the greater exothermicity of ethylene insertion into Zr−$CH_2CH_2CH_2Ph$ bonds versus Zr−C(benzyl) bonds results from the fact that the C(alkyl)−C(alkyl) bond formed is much stronger than the C(benzyl)−C(alkyl) bond formed.

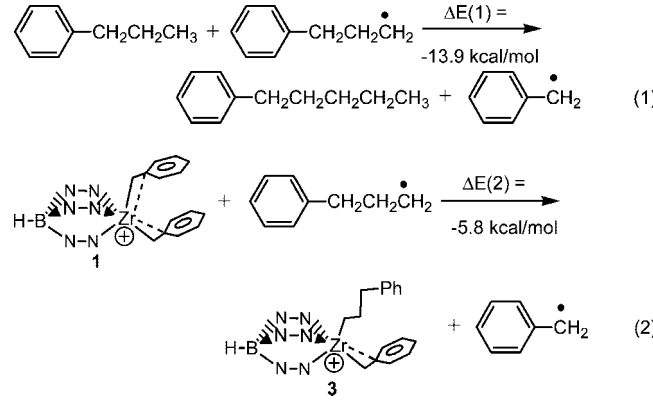

Similarly, the reaction energy for the isodesmic reaction in eq 4 shows that the Zr−$CH_2CH_2CH_2Ph$ bond in **6** is 3.3 kcal/mol stronger than the Zr−C(benzyl) bond in **3**. Therefore the conversion of **4** to **5** (Figure 2) is more exothermic than the conversion of **4** to **6** (Figure 4) primarily because the C(alkyl)−C(alkyl) bond formed in the former process is stronger than the C(benzyl)−C(alkyl) bond formed in the latter reaction.

(21) For comparison, the difference in bond dissociation energies for $PhCH_2$−Et (69 kcal/mol) and Et−Et (82 kcal/mol) is 13 kcal/mol. Sanderson, R. T. *Chemical Bonds and Bond Energies*; Academic: New York, 1976.

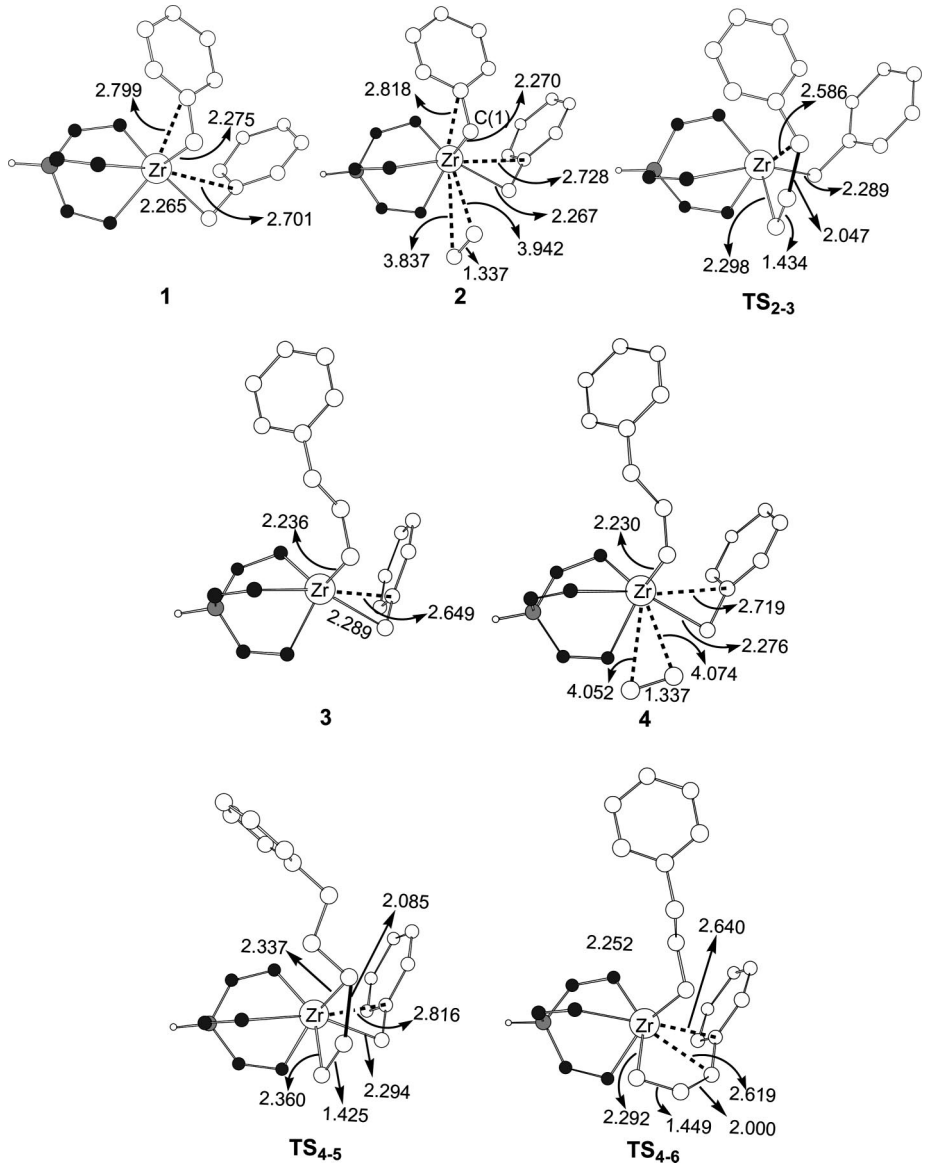

Figure 3. Selected bond distances (Å) calculated for species shown in Figure 2. For the purpose of clarity, the H atoms in the benzyl and ethylene ligands and the C and H atoms in the pyrazolyl rings of the Tp ligand are omitted.

The results in Figures 2, 4 and 5 also show that ethylene insertions into Zr−η^2-CH_2Ph bonds (**2** → **3**, **4** → **6**, and **8** → **9**) have higher barriers than insertions into Zr−$CH_2CH_2CH_2Ph$ bonds (**4** → **5** and **10** → **11**). Structural distortions of the Zr−η^2-CH_2Ph bonds of the migrating and spectator benzyl ligands contribute significantly to this trend. For example, Figure 3 shows that upon going from **2** to $\mathbf{TS_{2-3}}$, the migrating benzyl group slips to η^1-coordination and undergoes significant lengthening of the Zr−CH_2Ph bond ($\Delta d = 0.32$ Å), and the spectator benzyl ligand switches its coordination mode from η^2 to η^1. The spectator benzyl ligand in $\mathbf{TS_{2-3}}$ cannot maintain an η^2-coordination mode due to steric crowding with the migrating benzyl. Upon going from **4** to $\mathbf{TS_{4-6}}$, the migrating benzyl group also undergoes significant lengthening of the Zr−CH_2Ph bond ($\Delta d = 0.34$ Å). In contrast, upon going from **4** to $\mathbf{TS_{4-5}}$, the Zr−C bond of the migrating alkyl undergoes significantly less lengthening ($\Delta d = 0.11$ Å) and the η^2-coordination mode of the benzyl ligand is maintained. Similarly, Figure 6 shows that there is significantly greater structural distortion of the migrating benzyl group in the process **8** → $\mathbf{TS_{8-9}}$ compared to the migrating alkyl in the process **10** → $\mathbf{TS_{10-11}}$. In this case there is no spectator benzyl ligand involved, so the difference in the barriers between the two processes is smaller than for **2** → $\mathbf{TS_{2-3}}$ versus **4** → $\mathbf{TS_{4-5}}$. In general, benzyl migrations pass through later transition states, have higher barriers, and are less exothermic compared to alkyl migrations in these systems.

***β*-H Transfer Reactions.** Two important chain transfer processes in d^0 metal catalysts are β-H transfer to monomer via a six-centered transition state (BHT) and β-H elimination (BHE, i.e., β-H transfer to metal).[22] We investigated these pathways for Zr-butyl species derived from **1** and **7**.

Figure 7 shows the energy profile for β-H transfer to ethylene for Tp(CH_2Ph)Zr(^{n}Bu)($CH_2{=}CH_2$)$^+$ (**12**). The butyl group in **12** models the growing polymeryl chain formed by multiple ethylene insertions into **1**. The barrier for the BHT path **12** → $\mathbf{TS_{12-13}}$ → **13** (17.7 kcal/mol) is 6.3 kcal/mol higher than that for the preferred insertion path of **4** to produce **5** (Figure 2). The η^2-benzyl of **12** slips to η^1-coordination in $\mathbf{TS_{12-13}}$. We also attempted to calculate the barrier to β-H elimination of Tp(CH_2Ph)Zr(^{n}Bu)$^+$ (**14**, Scheme 4). However, the expected product, Tp(CH_2Ph)Zr(H)(butene)$^+$, does not correspond to a local minimum on the potential energy surface. Therefore neither the BHT nor the BHE chain transfer path is expected to compete

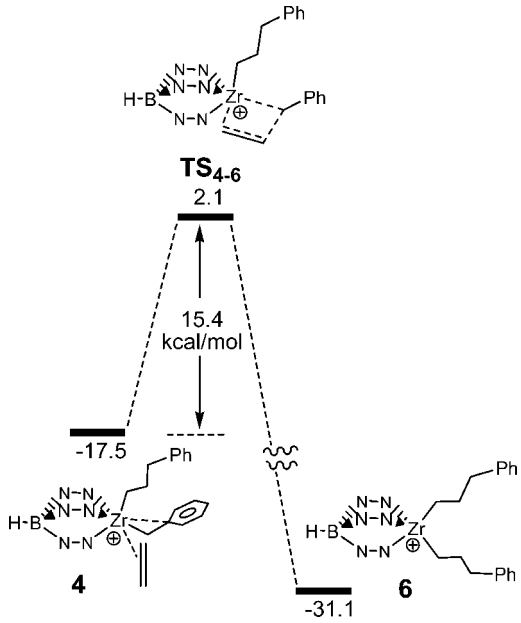

Figure 4. Calculated energy profile for ethylene insertion into the Zr−CH_2Ph bond of **4**. The relative electronic energies are given in kcal/mol.

with chain growth for catalyst **I**, which is consistent with the experimental results discussed above.

Figure 8 shows the energy profiles for β-H transfer to ethylene for {($PhCH_2$)(H)B(μ-pz)$_2$}(η^2-pz)Zr(^{n}Bu)(CH_2=CH_2)$^+$ (**15**). The calculated barrier for the BHT path **15** → **TS$_{15-16}$** → **16** (12.3 kcal/mol) is 2.3 kcal/mol higher than that for insertion of

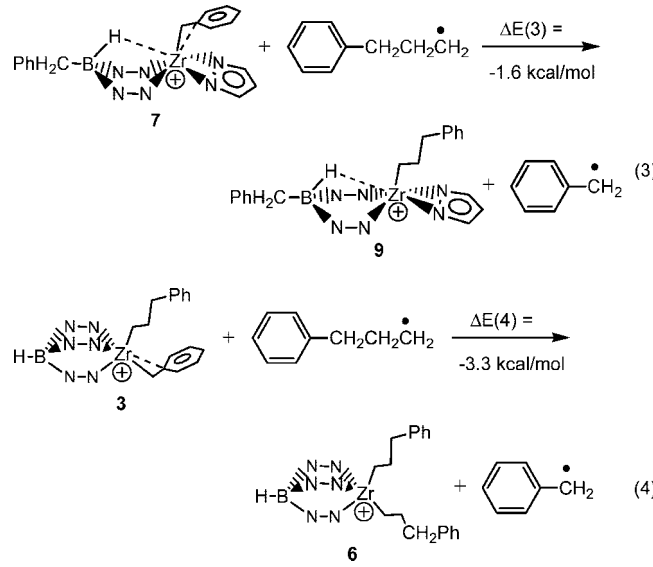

10. Figure 8 also shows that β-H elimination of Tp(CH_2Ph)Zr(^{n}Bu)$^+$ (**17**) to form Zr hydride species **18** has a very high barrier (22.0 kcal/mol) and is strongly endothermic ($\Delta E = -21.3$ kcal/mol). Therefore chain transfer via the BHT path may be possible for catalyst **II**, but the BHE path will not be important. This result is consistent with previous computational studies, which showed that BHT is preferred over BHE for group 4 metal catalysts.[22b] The short Zr−H bond distances in **TS$_{12-13}$** and **TS$_{15-16}$** (ca. 2.04 Å) indicate that the transferring hydrogen has significant bonding interaction with the metal center in both transition states.

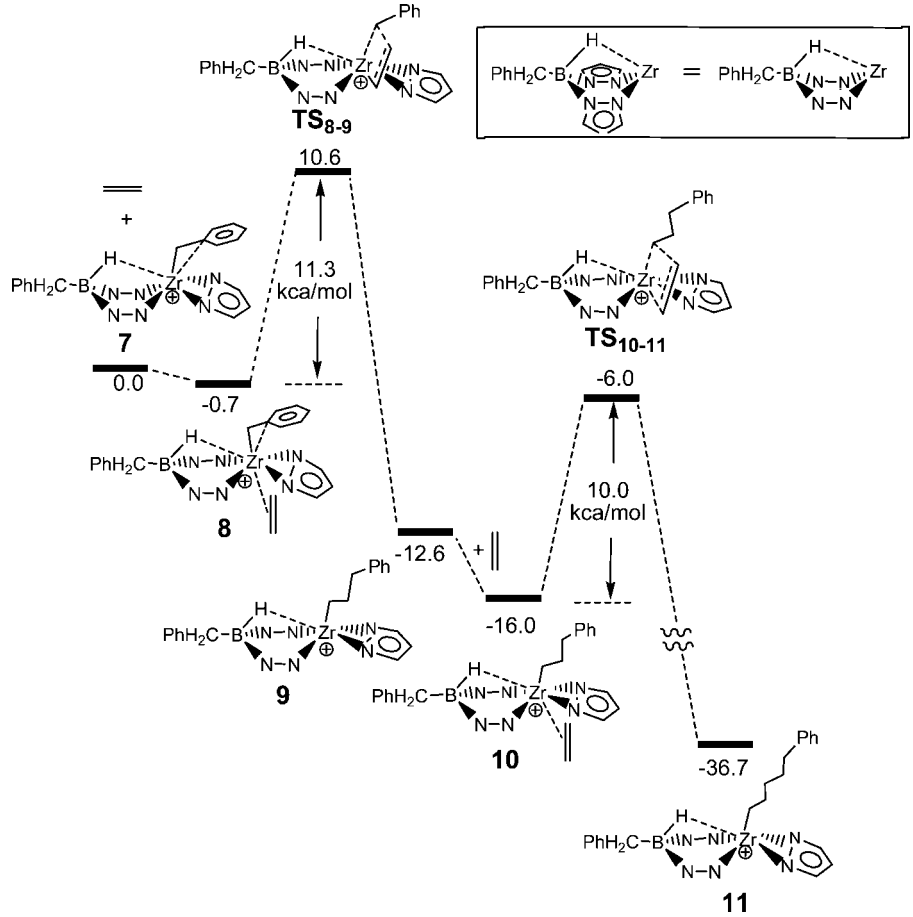

Figure 5. Calculated energy profile for the first two ethylene insertions of **7**. The relative electronic energies are given in kcal/mol.

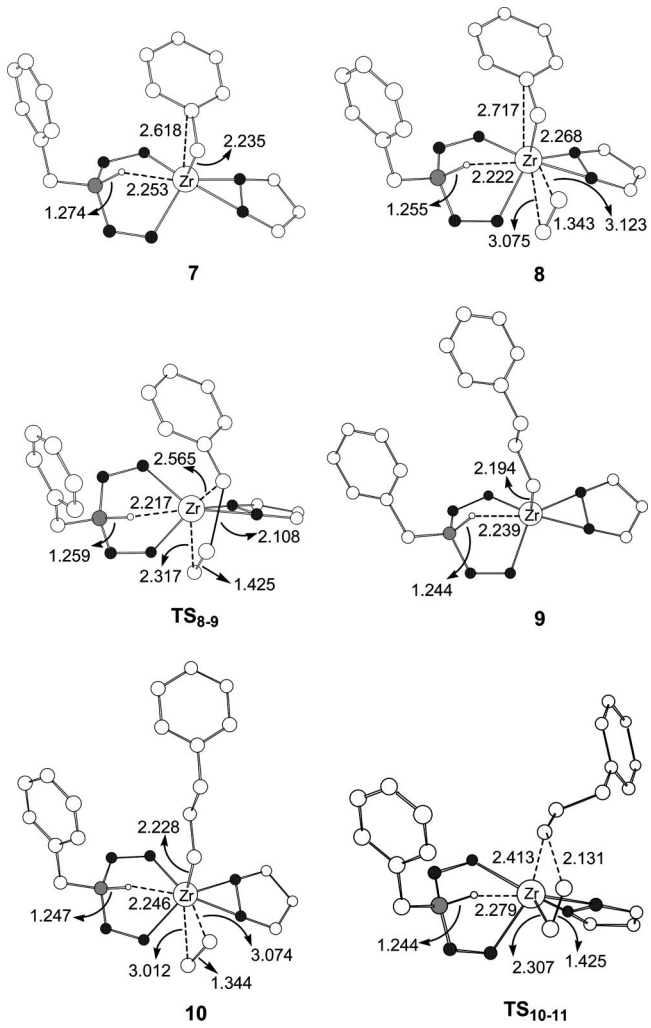

Figure 6. Selected bond distances (Å) calculated for species shown in Figure 5. For the purpose of clarity, the H atoms in the benzyl and ethylene ligands and the C and H atoms in the pyrazolyl rings of the Tp ligand are omitted.

Conclusion

The cationic complexes Tp*Zr(CH_2Ph)$_2^+$ (**I**) and {($PhCH_2$)(H)B(μ-Me_2pz)$_2$}Zr(η^2-Me_2pz)(CH_2Ph)$^+$ (**II**) polymerize ethylene at −78 to −60 °C to linear PE without significant chain transfer. For **I**, chain growth takes place at only one benzyl group. Quenching these polymerizations with MeOH yields benzyl-capped PE ($PhCH_2(CH_2CH_2)_nCH_2CH_3$). Quenching **I**-catalyzed ethylene polymerization with Br_2 yields double-end-capped PE containing benzyl and bromo end groups ($PhCH_2(CH_2CH_2)_nCH_2CH_2Br$). True living polymerization behavior is not observed for **I** and **II** because the first insertion (initiation) is slower than subsequent insertions (chain growth) and precipitation of the growing Zr-$(CH_2CH_2)_nCH_2CH_2Ph$ species results in mass transport limitations. DFT calculations on model catalysts show that ethylene insertion into a Zr−η^2-CH_2Ph bond requires greater structural distortion than insertion into a Zr−$CH_2CH_2CH_2Ph$ bond, which explains the observations that the first insertion is slower than subsequent insertions for **I** and **II** and chain growth occurs at only one benzyl ligand of **I**. The calculations also show that the β-H transfer to monomer and β-H elimination chain transfer pathways are both strongly disfavored for **I**, but the β-H transfer to monomer path may be possible for **II**.

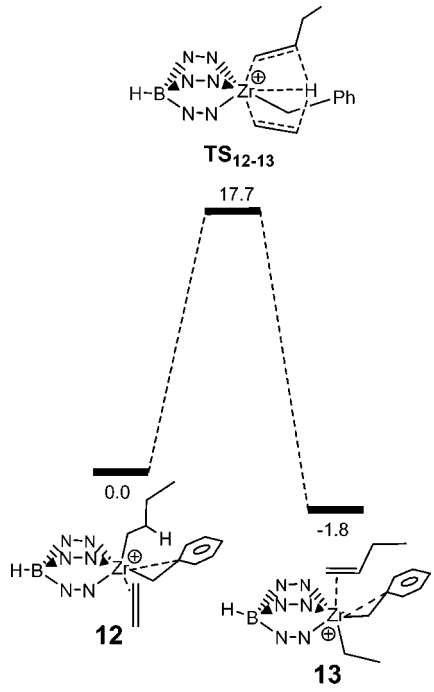

Figure 7. Calculated energy profile for β-hydrogen transfer to ethylene (BHT) of **12**. The relative electronic energies are given in kcal/mol.

Scheme 4

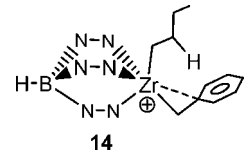

Experimental Section

General Procedures. All manipulations were carried out using vacuum line, Schlenk, or glovebox techniques under a purified N_2 atmosphere. Nitrogen was purified by passage through activated molecular sieves and Q-5 oxygen scavenger. CH_2Cl_2 and CD_2Cl_2 were degassed by freeze/pump/thaw cycles and dried over CaH_2 and/or P_2O_5. *o*-Dichlorobenzene-d_4 (Sigma-Aldrich), ethylene (99.999%, Matheson), and [Ph_3C][$B(C_6F_5)_4$] (Boulder Scientific) were used as received. Tp*Zr(CH_2Ph)$_3$ was prepared as described previously.[9]

NMR spectra of polyethylenes were recorded in *o*-dichlorobenzene-d_4 at 120 °C using a Bruker DRX 400 spectrometer (^{1}H: pulse width 90°, relaxation delay 30 s; ^{13}C: pulse width 90°, relaxation delay 0.1 s). ^{1}H chemical shifts were determined by reference to the residual ^{1}H solvent resonances and are reported relative to $SiMe_4$. ^{13}C chemical shifts were determined by reference to the PE main chain methylene peak (δ 30.0) and are reported relative to $SiMe_4$.[23] NMR samples were prepared by addition of ∼10 mg of the polymer to 0.7 g of *o*-dichlorobenzene-d_4 and were preheated at 100 °C to ensure complete dissolution.

DSC analyses were performed with a TA DSC-2920 differential scanning calorimeter. Samples were annealed by one cycle of heating to 200 °C and cooling to 0 at 5 °C/min and then analyzed at a heating rate of 10 °C/min.

(22) (a) Lohrenz, C. W.; Woo, T. K.; Fan, L.; Ziegler, T. *J. Organomet. Chem.* **1995**, *497*, 91. (b) Margl, P.; Deng, L.; Ziegler, T. *J. Am. Chem. Soc.* **1999**, *121*, 154. (c) Talarico, G.; Budzelaar, P. H. M. *J. Am. Chem. Soc.* **2006**, *128*, 4524.

(23) Barrera-Galland, G.; de Souza, R. F.; Santos-Mauler, R.; Nunes, F. F. *Macromolecules* **1999**, *32*, 1620.

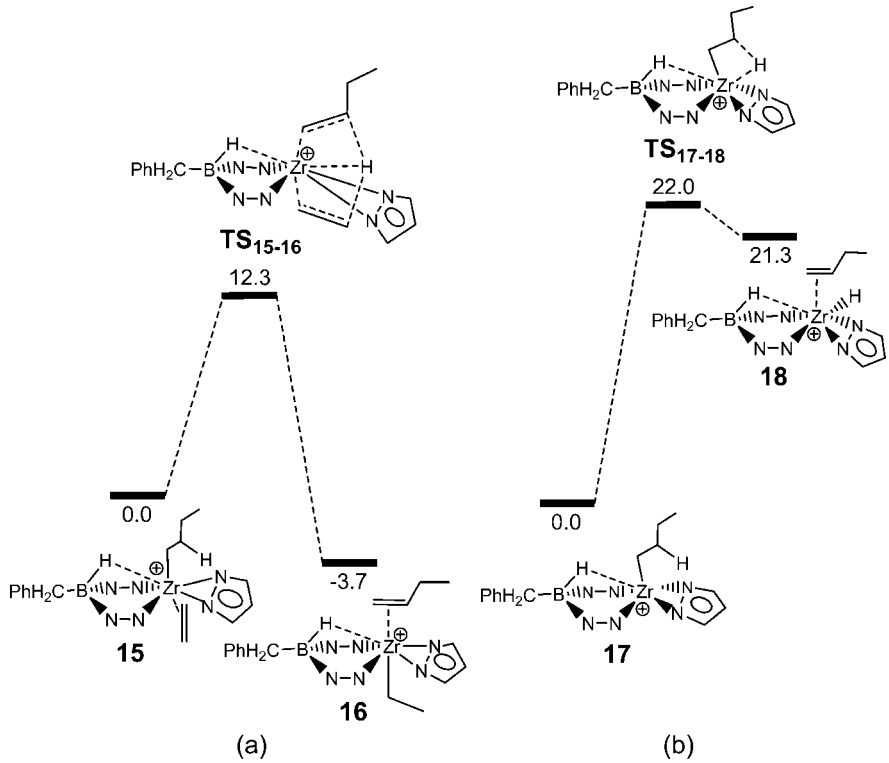

Figure 8. Calculated energy profiles for (a) β-hydrogen transfer to ethylene (BHT) of **15** and (b) β-hydrogen elimination (BHE) of **17**. The relative electronic energies are given in kcal/mol.

Ethylene Polymerization (NMR scale). A solution of **I** (10.8 μmol) in CD_2Cl_2 (0.59 mL) was prepared from Tp*Zr(CH_2Ph)$_3$ and [Ph_3C][$B(C_6F_5)_4$] (1 equiv) in an NMR tube at −60 °C. Ethylene (44 equiv) was added by vacuum transfer from a calibrated gas bulb at −196 °C. The tube was warmed to −78 °C, shaken vigorously at this temperature for ca. 1 min, and placed in a NMR probe that had been precooled to −60 °C. NMR spectra showed that 65% of **I** had been consumed based on the integrals of the CH_2Ph resonances of **I** and Ph_3CCH_2Ph (coproduct of the generation of **I**). The mixture was quenched by addition of methanol (1 mL) at −78 °C. The PE was collected by filtration. Similarly, a solution of **II** in CD_2Cl_2 was generated by warming a solution of **I** to 0 °C for 10 min. The solution was frozen at −196 °C and charged with ethylene (50 equiv vs Tp*Zr(CH_2Ph)$_3$), and the reaction was monitored and worked up as described for **I**. All of the ethylene and 74% of **II** were consumed and PE was formed.

Double-End-Capped Polyethylene. A flask equipped with a sidearm was charged with Tp*Zr(CH_2Ph)$_3$ (21.2 μmol) and [Ph_3C][$B(C_6F_5)_4$] (21.2 μmol) in a glovebox. The flask was sealed, removed from the glovebox, attached to a vacuum line, evacuated, and cooled to −78 °C. Dichloromethane (20 mL) was added by vacuum transfer, and the mixture was stirred vigorously. Under these conditions **I** and Ph_3CCH_2Ph are formed quantitatively. The flask was maintained at −78 °C for 5 min and then exposed to ethylene at a constant pressure of 1 atm. After the desired reaction time (usually ca. 2 min), excess Br_2 was added through the sidearm via syringe while the ethylene pressure was maintained. The mixture was stirred for a few minutes, and the flask was warmed to room temperature and vented. The polymer was collected by filtration, washed with methanol, acetone, and hexane, and dried under vacuum for 12 h.

Molecular Weight Determination. Number average molecular weights were determined by ^{1}H NMR. **$PhCH_2(CH_2)_nCH_3$**: In the absence of chain transfer, each molecule of **I** or **II** that reacts with ethylene produces one polymer chain, assuming that insertion into only one Zr−CH_2Ph bond of **I** occurs. In this case, the expected M_n ($M_{n,calcd}$) is given by eq 5, in which n_{Zr} is the number of moles of **I** or **II** that is consumed, $n_{ethylene}$ is the number of moles of ethylene that is consumed, and 92 is the sum of the molecular weights of the −CH_2Ph and −H chain ends. $M_{n,NMR}$ was determined by eqs 6 and 7, in which X_n is the average degree of polymerization (the average number of monomer units per chain), I_{CH2} is the sum of integrals of the main chain and penultimate −CH_2− resonances, and I_{CH3} is the integral of −CH_3 resonance.

$$M_{n,calcd} = (28n_{ethylene}+92n_{Zr})/n_{Zr} \quad (5)$$

$$M_{n,NMR} = 92 + 28X_n \quad (6)$$

$$X_n = \{(I_{CH2}/2) + (I_{CH3}/3)\}/\{2I_{CH3}/3)\} \quad (7)$$

$PhCH_2(CH_2)_nCH_2Br$. $M_{n,NMR}$ values for double-end-capped PEs were determined by eqs 8 and 9, in which I_{CH2} is the sum of integrals of the main chain and penultimate −CH_2− resonances and I_{CH2Br} and I_{CH2Ph} are the integrals of the −CH_2Br and −CH_2Ph resonances, respectively.

$$M_{n,NMR} = 28X_n + 91.1 + 79.9 \quad (8)$$

$$X_n = (I_{CH2}+I_{CH2Br})/2I_{CH2Ph} \quad (9)$$

Computational Details. Molecular geometries of the model complexes were optimized without constraints at the Becke3LYP (B3LYP) level of density functional theory.[24] Frequency calculations at the same level of theory were also performed to characterize the stationary points as minima (zero imaginary frequencies) or transition states (one imaginary frequency). The effective core potentials of Hay and Wadt with a double-ζ valance basis set (LanL2DZ) were used for Zr.[25] The 6-31G basis set was used for C, H, N, and B.[26] The basis sets for the carbon atoms of ethylene

(24) (a) Lee, C.; Yang, W.; Parr, G. *Phys. Rev.* **1988**, *B37*, 785. (b) Miehlich, B.; Savin, A.; Stoll, H.; Preuss, H. *Chem. Phys. Lett.* **1989**, *157*, 200. (c) Becke, A. D. *J. Chem. Phys.* **1993**, *98*, 5648.

(25) (a) Hay, P. J.; Wadt, W. R. *J. Chem. Phys.* **1985**, *82*, 70. (b) Wadt, W. R.; Hay, P. J. *J. Chem. Phys.* **1985**, *82*, 284. (c) Hay, P. J.; Wadt, W. R. *J. Chem. Phys.* **1985**, *82*, 299.

and CH_2 unit of the benzyl groups were augmented by the polarization function $\zeta_d = 0.6$.[27] This basis set is referred to as BS1. The relative energies shown in the energy profiles were obtained by single-point energy calculations with improved basis sets (BS2) as defined here: BS2 replaces the basis set of 6-31G in BS1 with 6-31G** and includes *f* polarization functions ($\zeta_f = 0.875$) for Zr.[28] Calculations were performed with the Gaussian 03 software package.[29]

Acknowledgment. This work was supported by the U.S. Department of Energy (DE-FG-02-00ER15036), the U.S. National Science Foundation (CHE-0516950), and the Research Grant Council of Hong Kong (HKUST 601507).

Supporting Information Available: Additional NMR data, the complete citation for ref 29, and tables giving Cartesian coordinates and electronic energies for all of the calculated structures. This material is available free of charge via the Internet at http://pubs.acs.org.

OM800558W

(26) Hariharan, P. C.; Pople, J. A. *Theor. Chim. Acta* **1973**, *28*, 213.
(27) Huzinaga, S. *Gaussian Basis Sets for Molecular Calculations*; Elsevier: Amsterdam, 1984.
(28) Ehlers, A. W.; Bohme, M.; Dapprich, S.; Gobbi, A.; Hollwarth, A.; Jonas, V.; Kohler, K. F.; Stegmann, R.; Veldkamp, A.; Frenking, G. *Chem. Phys. Lett.* **1993**, *208*, 111.
(29) Frisch, M. J.; et al. *Gaussian 03*, revision B05; Gaussian, Inc.: Pittsburgh, PA, 2003.